УДК 538.945

Band Structure Modification Due to the Spin-orbit Coupling in the Three-orbital Model for Iron Pnictides

Maxim M. Korshunov*
Siberian Federal University
Svobodny, 79, Krasnoyarsk, 660041
Kirensky Institute of Physics
Federal Research Center KSC SB RAS
Akademgorodok, Krasnoyarsk, 660036
Russia

Yuliya N. Togushova†
Siberian Federal University
Svobodny, 79, Krasnoyarsk, 660041
Russia

Received 19.11.2017, received in revised form 21.11.2017, accepted 20.04.2018

We study the effect of the spin-orbit coupling on the band structure and the Fermi surface of the three-orbital model within the two-iron Brillouin zone. Due to the presence of two irons in the crystallographically correct unit cell, the spin-orbit coupling can be divided into the intra- and intercell parts with respect to the one-iron unit cell. We show that the intercell part produces the reconstruction of the Fermi surface in the form of the pronounced splitting between the previously degenerate electron (π, π)-pockets along the $(0, \pi) - (\pi, \pi)$ direction. Intracell part shifts the bands around $(0, 0)$ point and removes degeneracy there. There are also some other band shifts but they should not affect the low-energy physics because they occur at energy scales of about 1 eV below the Fermi level.

Keywords: Fe-based superconductors, spin-orbit coupling, band structure, Fermi surface.
DOI: 10.17516/1997-1397-2018-11-4-430-437.

Discovery of superconductivity in iron-based systems in 2008 revived the interest in multi-band systems [1]. Fermi surface in iron pnictides is formed by at least three bands. According to the density-functional studies (DFT) within LDA (local-density approximation) and GGA (generalized gradient approximation) and ARPES (angle-resolved photo-emission spectroscopy), thee bands originate from the three t_{2g} iron d-orbitals. That is, the hybridization of the xz, yz, and xy orbitals results in two electron-like Fermi surface pockets around $X = (\pi, 0)$ and $Y = (0, \pi)$ points and one hole-like pocket around $\Gamma = (0, 0)$ point in the 1-Fe Brillouin zone. Nesting between two groups of sheets is the driving force for the spin-density wave antiferromagnetic order in the undoped systems [2]. The scattering with the wave vector connecting hole and electron pockets is the most probable candidate for the superconducting pairing in the doped systems. In particular, the spin-fluctuation approach result the extended s-wave gap which changes sign between hole and electron sheets ($s_{\pm}$ state [3]) as the leading instability [1, 4–7].

There are several low-energy models for iron pnictides. Simplest one is the two-orbital model [8] correctly describing the dominant d_{xz}-d_{yz} contribution to the Fermi surface. It has

*mkor@iph.krasn.ru
†ytogushova@sfu-kras.ru

many disadvantages including misplacement of the second hole pocket, wrong Fermi velocities as compared with ARPES and DFT, and absence of d_{xy} orbital contribution which is known to appear near or even at the Fermi level (both ARPES and DFT). Here we use the three-orbital model from Ref. [9] that comes from the t_{2g} manifold. In particular, there the d_{xz} and d_{yz} orbitals are hybridized to form two electron Fermi surface sheets around X and Y points and one hole sheet around Γ point of the 1-Fe Brillouin zone (1-Fe BZ). The d_{xy} orbital is decoupled from the others and form an outer hole pocket around Γ point.

One of the puzzles in iron-based superconductors is the anisotropy of the spin resonance peak [10]. It was found that transverse and longitudinal components of the spin susceptibility, χ_{+-} and $2\chi_{zz}$, violate the spin-rotational invariance, $\langle S_+S_-\rangle = 2\langle S_zS_z\rangle$. Later have to be obeyed in the disordered system. One of the solution to the puzzle is the effect of the spin-orbit (SO) interaction that can break the spin-rotational invariance like it does in Sr_2RuO_4 [11]. This approach was used before to study the spin response in model from Ref. [9] within the 1-Fe BZ [12].

There is a complication coming from the As, which forms square lattice planes between the lattice sites of, but also above and below, the square lattice of Fe. This alternating pattern of As makes the correct real space unit cell twice the 1-Fe unit cell. The corresponding 2-Fe BZ is twice as small as the 1-Fe one and called "folded BZ". For the simplest case of single-layer Fe pnictides the folding wave vector is two-dimensional and equal to $\mathbf{Q}_F = (\pi, \pi)$. Most experimental results and DFT band structure are reported in the folded BZ since crystallographically it is the correct one. However, some experiments sensitive to the Fe positions, like neutron scattering on Fe moments, have more meaning in the 1-Fe BZ ("unfolded" zone).

Here we study the role of the SO coupling in the formation of the band structure and the Fermi surface in the 2-Fe BZ within the three-orbital model from Ref. [9].

1. Three-orbital model in 1-Fe BZ

We write the Hamiltonian of the three-orbital model [9] in the following form:

$$H_0 = \sum_{\mathbf{k},\sigma,l,m} \varepsilon_{\mathbf{k}}^{lm} c_{\mathbf{k}l\sigma}^{\dagger} c_{\mathbf{k}m\sigma}, \tag{1}$$

where l and m are orbital indices, $c_{\mathbf{k}m\sigma}$ is the annihilation operator of a particle with momenta $\mathbf{k}$ and a spin σ. We choose the following numbering of orbitals, $d_{xy} \leftrightarrow 1, d_{yz} \leftrightarrow 2, d_{zx} \leftrightarrow 3$. The model consists of the three t_{2g} orbitals and all of them are hybridized. Matrix of one-electron energies and hoppings, $\hat{\varepsilon}_{\mathbf{k}}$, is given by

$$\hat{\varepsilon}_{\mathbf{k}} = \begin{pmatrix} \varepsilon_{1\mathbf{k}} & 0 & 0 \\ 0 & \varepsilon_{2\mathbf{k}} & \varepsilon_{4\mathbf{k}} \\ 0 & \varepsilon_{4\mathbf{k}} & \varepsilon_{3\mathbf{k}} \end{pmatrix}, \tag{2}$$

where $\varepsilon_{1\mathbf{k}} = \epsilon_{xy} - \mu + 2t_{xy}(\cos k_x + \cos k_y) + 4t'_{xy} \cos k_x \cos k_y$, $\varepsilon_{2\mathbf{k}} = \epsilon_{yz} - \mu + 2t_x \cos k_x + 2t_y \cos k_y + 4t' \cos k_x \cos k_y + 2t''(\cos 2k_x + \cos 2k_y)$, $\varepsilon_{3\mathbf{k}} = \epsilon_{xz} - \mu + 2t_y \cos k_x + 2t_x \cos k_y + 4t' \cos k_x \cos k_y + 2t''(\cos 2k_x + \cos 2k_y)$, $\varepsilon_{4\mathbf{k}} = 4t_{xzyz} \sin k_x/2 \sin k_y/2$. The following set of parameters (in eV) allows to reproduce the topology of the Fermi surface in iron pnictides: chemical potential $\mu = 0$, $\epsilon_{xy} = -0.70$, $\epsilon_{yz} = -0.34$, $\epsilon_{xz} = -0.34$, $t_{xy} = 0.18$, $t'_{xy} = 0.06$, $t_x = 0.26$, $t_y = -0.22$, $t' = 0.2$, $t'' = -0.07$, $t_{xzyz} = 0.38$.

2. Spin-orbit coupling in 1-Fe BZ

Following Ref. [13], we write the spin-orbit coupling terms, $H_{SO} = \lambda \sum_f \mathbf{L}_f \cdot \mathbf{S}_f$, in the second-quantized form assuming that three t_{2g} states behave like an $\ell = 1$ angular momentum representation,

$$H_{SO} = \mathrm{i}\frac{\lambda}{2} \sum_{l,m,n} \epsilon_{lmn} \sum_{\mathbf{k},\sigma,\sigma'} c^\dagger_{\mathbf{k}l\sigma} c_{\mathbf{k}m\sigma'} \hat{\sigma}^n_{\sigma\sigma'}, \tag{3}$$

where ϵ_{lmn} is the completely antisymmetric tensor, indices $\{l, m, n\}$ take values $\{x, y, z\}$ or equivalently $\{x, y, z\} \leftrightarrow \{d_{yz}, d_{zx}, d_{xy}\} \leftrightarrow \{2, 3, 1\}$, and $\hat{\sigma}^n_{\sigma\sigma'}$ are the Pauli spin matrices. Explicit form of the Hamiltonian is the following:

$$H_{SO} = \mathrm{i}\frac{\lambda}{2} \sum_{\mathbf{k},\sigma} \left[c^\dagger_{\mathbf{k}2\sigma} c_{\mathbf{k}3\sigma} \mathrm{sgn}\,(\sigma) + \mathrm{i} c^\dagger_{\mathbf{k}2\sigma} c_{\mathbf{k}1\bar{\sigma}} \mathrm{sgn}\,(\sigma) + c^\dagger_{\mathbf{k}3\sigma} c_{\mathbf{k}1\bar{\sigma}} - h.c. \right], \tag{4}$$

Let us introduce vector operators in the orbital space, $\hat{\Psi}^\dagger_{\mathbf{k}\sigma} = \left(c^\dagger_{\mathbf{k}1\sigma}, c^\dagger_{\mathbf{k}2\sigma}, c^\dagger_{\mathbf{k}3\sigma} \right)$. Then,

$$H_0 = \sum_{\mathbf{k},\sigma} \hat{\Psi}^\dagger_{\mathbf{k}\sigma} \hat{\varepsilon}_{\mathbf{k}} \hat{\Psi}_{\mathbf{k}\sigma}, \; H_{SO} = \sum_{\mathbf{k},\sigma,\sigma'} \hat{\Psi}^\dagger_{\mathbf{k}\sigma} \hat{\varepsilon}^{\sigma\sigma'}_{SO} \hat{\Psi}_{\mathbf{k}\sigma'}. \tag{5}$$

Here

$$\hat{\varepsilon}^{\sigma\sigma'}_{SO} = \mathrm{i}\frac{\lambda}{2} \begin{pmatrix} 0 & -\mathrm{i}\delta_{\sigma',\bar{\sigma}} \mathrm{sgn}\,(\sigma) & \delta_{\sigma',\bar{\sigma}} \\ \mathrm{i}\delta_{\sigma',\bar{\sigma}} \mathrm{sgn}\,(\sigma) & 0 & \delta_{\sigma',\sigma} \mathrm{sgn}\,(\sigma) \\ -\delta_{\sigma',\bar{\sigma}} & -\delta_{\sigma',\sigma} \mathrm{sgn}\,(\sigma) & 0 \end{pmatrix} = \tag{6}$$

$$= \mathrm{i}\frac{\lambda}{2} \left[\hat{\varepsilon}^z \delta_{\sigma',\sigma} \mathrm{sgn}\,(\sigma) + \delta_{\sigma',\bar{\sigma}} \left(\hat{\varepsilon}^x - \mathrm{i}\hat{\varepsilon}^y \mathrm{sgn}\,(\sigma) \right) \right], \tag{7}$$

where we have introduces the following matrices:

$$\hat{\varepsilon}^z = \begin{pmatrix} 0 & 0 & 0 \\ 0 & 0 & 1 \\ 0 & -1 & 0 \end{pmatrix} = \mathrm{i}J_x, \hat{\varepsilon}^x = \begin{pmatrix} 0 & 0 & 1 \\ 0 & 0 & 0 \\ -1 & 0 & 0 \end{pmatrix} = -\mathrm{i}J_y, \hat{\varepsilon}^y = \begin{pmatrix} 0 & 1 & 0 \\ -1 & 0 & 0 \\ 0 & 0 & 0 \end{pmatrix} = \mathrm{i}J_z. \tag{8}$$

Here, J_i are the generators of the rotation group $O(3)$. It is well known [14] that $O(3)$ transformation of the (x, y, z) vector is equivalent to the $SU(2)$ transformation of the (ξ_1, ξ_2) spinor if $x = \frac{1}{2}(\xi_2^2 - \xi_1^2),\; y = \frac{1}{2\mathrm{i}}(\xi_2^2 + \xi_1^2),\; z = \xi_1\xi_2$.

The total Hamiltonian $H = H_0 + H_{SO}$ can be written explicitly as

$$H = \sum_{\mathbf{k},\sigma} \left[\hat{\Psi}^\dagger_{\mathbf{k}\sigma} \left(\hat{\varepsilon}_{\mathbf{k}} + \mathrm{i}\frac{\lambda}{2} \hat{\varepsilon}^z \mathrm{sgn}\,(\sigma) \right) \hat{\Psi}_{\mathbf{k}\sigma} + \mathrm{i}\frac{\lambda}{2} \hat{\Psi}^\dagger_{\mathbf{k}\sigma} \left(\hat{\varepsilon}^x - \mathrm{i}\hat{\varepsilon}^y \mathrm{sgn}\,(\sigma) \right) \hat{\Psi}_{\mathbf{k}\bar{\sigma}} \right] =$$

$$= \sum_{\mathbf{k}} \left[\hat{\Psi}^\dagger_{\mathbf{k}\uparrow} \left(\hat{\varepsilon}_{\mathbf{k}} + \mathrm{i}\frac{\lambda}{2} \hat{\varepsilon}^z \right) \hat{\Psi}_{\mathbf{k}\uparrow} + \hat{\Psi}^\dagger_{\mathbf{k}\downarrow} \left(\hat{\varepsilon}_{\mathbf{k}} - \mathrm{i}\frac{\lambda}{2} \hat{\varepsilon}^z \right) \hat{\Psi}_{\mathbf{k}\downarrow} + \right.$$

$$\left. + \mathrm{i}\frac{\lambda}{2} \hat{\Psi}^\dagger_{\mathbf{k}\uparrow} \hat{\varepsilon}^x \hat{\Psi}_{\mathbf{k}\downarrow} + \mathrm{i}\frac{\lambda}{2} \hat{\Psi}^\dagger_{\mathbf{k}\downarrow} \hat{\varepsilon}^x \hat{\Psi}_{\mathbf{k}\uparrow} + \frac{\lambda}{2} \hat{\Psi}^\dagger_{\mathbf{k}\uparrow} \hat{\varepsilon}^y \hat{\Psi}_{\mathbf{k}\downarrow} - \frac{\lambda}{2} \hat{\Psi}^\dagger_{\mathbf{k}\downarrow} \hat{\varepsilon}^y \hat{\Psi}_{\mathbf{k}\uparrow} \right] =$$

$$= \sum_{\mathbf{k}} \begin{pmatrix} \hat{\Psi}^\dagger_{\mathbf{k}\uparrow} & \hat{\Psi}^\dagger_{\mathbf{k}\downarrow} \end{pmatrix} \cdot \hat{H} \cdot \begin{pmatrix} \hat{\Psi}_{\mathbf{k}\uparrow} \\ \hat{\Psi}_{\mathbf{k}\downarrow} \end{pmatrix}, \tag{9}$$

where

$$\hat{H} = \begin{pmatrix} \hat{\varepsilon}_{\mathbf{k}} + \mathrm{i}\frac{\lambda}{2} \hat{\varepsilon}^z & \mathrm{i}\frac{\lambda}{2} \hat{\varepsilon}^x + \frac{\lambda}{2} \hat{\varepsilon}^y \\ \mathrm{i}\frac{\lambda}{2} \hat{\varepsilon}^x - \frac{\lambda}{2} \hat{\varepsilon}^y & \hat{\varepsilon}_{\mathbf{k}} - \mathrm{i}\frac{\lambda}{2} \hat{\varepsilon}^z \end{pmatrix}. \tag{10}$$

If one considers only the z-component of the SO coupling, then the expression for H simplifies significantly,

$$H_z = H_0 + H_{SOz} = \sum_{\mathbf{k},\sigma} \hat{\Psi}^{\dagger}_{\mathbf{k}\sigma} \left(\hat{\varepsilon}_{\mathbf{k}} + \mathrm{i}\frac{\lambda}{2}\hat{\varepsilon}^z \mathrm{sgn}\,(\sigma) \right) \hat{\Psi}_{\mathbf{k}\sigma} = \sum_{\mathbf{k}} \begin{pmatrix} \hat{\Psi}^{\dagger}_{\mathbf{k}\uparrow} & \hat{\Psi}^{\dagger}_{\mathbf{k}\downarrow} \end{pmatrix} \cdot \hat{H}_z \cdot \begin{pmatrix} \hat{\Psi}_{\mathbf{k}\uparrow} \\ \hat{\Psi}_{\mathbf{k}\downarrow} \end{pmatrix}, \quad (11)$$

where

$$\hat{H}_z = \begin{pmatrix} \hat{\varepsilon}_{\mathbf{k}} + \mathrm{i}\frac{\lambda}{2}\hat{\varepsilon}^z & 0 \\ 0 & \hat{\varepsilon}_{\mathbf{k}} - \mathrm{i}\frac{\lambda}{2}\hat{\varepsilon}^z \end{pmatrix}. \quad (12)$$

Therefore, z-component of the SO interaction modifies one-electron energies only, but does it differently for spin-up and spin-down elements of the spin-resolved Hamiltonian matrix $\hat{H}$. On the other hand, x- and y-components mix spin-up and spin-down matrix elements and thus effectively increase the dimensionality of the problem by a factor of two.

3. Spin-orbit coupling in 2-FeBZ

While working in the unfolded BZ as before, we are missing important effect of the SO hybridization between orbitals on neighboring irons. After such a hybridization the unfolding is not possible any more. Hereafter we utilize the following conjecture: the structure of the SO coupling between two orbitals on neighboring irons is the same as the structure between two orbitals with the same symmetry on the one iron. Thus, if SO coupling between d_{xz} and d_{yz} orbitals has the form $\mathrm{i}\frac{\lambda}{2}\hat{\varepsilon}^z$, the same form holds for d_{xz} on Fe-1 (some one-iron unit cell) and d_{yz} on Fe-2 (neighboring one-iron unit cell). For convenience, we assign different coupling constant, λ', to intercell SO interaction; one can always put it to be equal to λ. Note that when we use a wording 'intercell SO coupling', it does not mean a long-range SO coupling. The SO interaction is always local but since orbitals of two neighboring irons hybridize directly and through As, the wave functions of electrons on these orbitals can overlap that opens up a possibility for the effectively intercell SO coupling.

Brillouin zone folding, i.e. transition from 1-Fe BZ to 2-Fe BZ, is done in two steps. First, momenta are transformed as $(k_x + k_y)/2 \to k'_x$, $(k_x - k_y)/2 \to k'_y$. Second, the Hamiltonian matrix is doubled by adding the shifted $\varepsilon^{lm}_{\mathbf{k}'+\mathbf{Q}_F}$, where $\mathbf{Q}_F = (\pi, \pi)$ is the folding wave vector. Thus, the Hamiltonian (1) takes the form

$$H_0 = \sum_{\mathbf{k}',\sigma,l,m} \varepsilon^{lm}_{\mathbf{k}'} c^{\dagger}_{\mathbf{k}'l\sigma} c_{\mathbf{k}'m\sigma} + \sum_{\mathbf{k}',\sigma,l,m} \varepsilon^{lm}_{\mathbf{k}'+\mathbf{Q}_F} c^{\dagger}_{\mathbf{k}'+\mathbf{Q}_F l\sigma} c_{\mathbf{k}+\mathbf{Q}_F m\sigma}. \quad (13)$$

Later we skip prime assuming that all momenta are within the 2-Fe BZ.

The Hamiltonian can be written in the matrix form analogous to Eq. (9),

$$H = \sum_{\mathbf{k}} \begin{pmatrix} \hat{\Psi}^{\dagger}_{\mathbf{k}\uparrow} & \hat{\Psi}^{\dagger}_{\mathbf{k}\downarrow} & \hat{\Phi}^{\dagger}_{\mathbf{k}\uparrow} & \hat{\Phi}^{\dagger}_{\mathbf{k}\downarrow} \end{pmatrix} \cdot \hat{H} \cdot \begin{pmatrix} \hat{\Psi}_{\mathbf{k}\uparrow} \\ \hat{\Psi}_{\mathbf{k}\downarrow} \\ \hat{\Phi}_{\mathbf{k}\uparrow} \\ \hat{\Phi}_{\mathbf{k}\downarrow} \end{pmatrix}, \quad (14)$$

where $\hat{\Psi}_{\mathbf{k}\sigma}$ ($\hat{\Phi}_{\mathbf{k}\sigma}$) corresponds to the first (second) set of iron orbitals.

In case of intracell SO coupling, $\hat{H}$ has the form which immediately follows from Eq. (10):

$$\hat{H} = \left(\begin{array}{cc|cc} \hat{\varepsilon}_{\mathbf{k}} + \mathrm{i}\frac{\lambda}{2}\hat{\varepsilon}^z & \mathrm{i}\frac{\lambda}{2}\hat{\varepsilon}^x + \frac{\lambda}{2}\hat{\varepsilon}^y & 0 & 0 \\ \mathrm{i}\frac{\lambda}{2}\hat{\varepsilon}^x - \frac{\lambda}{2}\hat{\varepsilon}^y & \hat{\varepsilon}_{\mathbf{k}} - \mathrm{i}\frac{\lambda}{2}\hat{\varepsilon}^z & 0 & 0 \\ \hline 0 & 0 & \hat{\varepsilon}_{\mathbf{k}+\mathbf{Q}_F} + \mathrm{i}\frac{\lambda}{2}\hat{\varepsilon}^z & \mathrm{i}\frac{\lambda}{2}\hat{\varepsilon}^x + \frac{\lambda}{2}\hat{\varepsilon}^y \\ 0 & 0 & \mathrm{i}\frac{\lambda}{2}\hat{\varepsilon}^x - \frac{\lambda}{2}\hat{\varepsilon}^y & \hat{\varepsilon}_{\mathbf{k}+\mathbf{Q}_F} - \mathrm{i}\frac{\lambda}{2}\hat{\varepsilon}^z \end{array}\right). \tag{15}$$

For finite λ, the result of diagonalization of Eq. (15) is the same as of Eq. (10). New effects come in once we add the intercell SO coupling:

$$\hat{H}_{SOinter} = \left(\begin{array}{cc|cc} 0 & 0 & \mathrm{i}\frac{\lambda'}{2}\hat{\varepsilon}^z & \mathrm{i}\frac{\lambda'}{2}\hat{\varepsilon}^x + \frac{\lambda'}{2}\hat{\varepsilon}^y \\ 0 & 0 & \mathrm{i}\frac{\lambda'}{2}\hat{\varepsilon}^x - \frac{\lambda'}{2}\hat{\varepsilon}^y & -\mathrm{i}\frac{\lambda'}{2}\hat{\varepsilon}^z \\ \hline \mathrm{i}\frac{\lambda'}{2}\hat{\varepsilon}^z & \mathrm{i}\frac{\lambda'}{2}\hat{\varepsilon}^x + \frac{\lambda'}{2}\hat{\varepsilon}^y & 0 & 0 \\ \mathrm{i}\frac{\lambda'}{2}\hat{\varepsilon}^x - \frac{\lambda'}{2}\hat{\varepsilon}^y & -\mathrm{i}\frac{\lambda'}{2}\hat{\varepsilon}^z & 0 & 0 \end{array}\right). \tag{16}$$

The total Hamiltonian is given by the sum of matrices (15) and (16),

$$\hat{H} = \left(\begin{array}{cc|cc} \hat{\varepsilon}_{\mathbf{k}} + \mathrm{i}\frac{\lambda}{2}\hat{\varepsilon}^z & \mathrm{i}\frac{\lambda}{2}\hat{\varepsilon}^x + \frac{\lambda}{2}\hat{\varepsilon}^y & \mathrm{i}\frac{\lambda'}{2}\hat{\varepsilon}^z & \mathrm{i}\frac{\lambda'}{2}\hat{\varepsilon}^x + \frac{\lambda'}{2}\hat{\varepsilon}^y \\ \mathrm{i}\frac{\lambda}{2}\hat{\varepsilon}^x - \frac{\lambda}{2}\hat{\varepsilon}^y & -\mathrm{i}\frac{\lambda'}{2}\hat{\varepsilon}^z & \mathrm{i}\frac{\lambda'}{2}\hat{\varepsilon}^x - \frac{\lambda'}{2}\hat{\varepsilon}^y & -\mathrm{i}\frac{\lambda'}{2}\hat{\varepsilon}^z \\ \hline \mathrm{i}\frac{\lambda'}{2}\hat{\varepsilon}^z & \mathrm{i}\frac{\lambda'}{2}\hat{\varepsilon}^x + \frac{\lambda'}{2}\hat{\varepsilon}^y & \hat{\varepsilon}_{\mathbf{k}+\mathbf{Q}_F} + \mathrm{i}\frac{\lambda'}{2}\hat{\varepsilon}^z & \mathrm{i}\frac{\lambda}{2}\hat{\varepsilon}^x + \frac{\lambda}{2}\hat{\varepsilon}^y \\ \mathrm{i}\frac{\lambda'}{2}\hat{\varepsilon}^x - \frac{\lambda'}{2}\hat{\varepsilon}^y & -\mathrm{i}\frac{\lambda'}{2}\hat{\varepsilon}^z & \mathrm{i}\frac{\lambda'}{2}\hat{\varepsilon}^x - \frac{\lambda}{2}\hat{\varepsilon}^y & \hat{\varepsilon}_{\mathbf{k}+\mathbf{Q}_F} - \mathrm{i}\frac{\lambda}{2}\hat{\varepsilon}^z \end{array}\right). \tag{17}$$

Again, if one considers only z-component of the SO coupling, the expression for H simplifies:

$$\hat{H} \to \hat{H}_z = \left(\begin{array}{cc|cc} \hat{\varepsilon}_{\mathbf{k}} + \mathrm{i}\frac{\lambda}{2}\hat{\varepsilon}^z & 0 & \mathrm{i}\frac{\lambda'}{2}\hat{\varepsilon}^z & 0 \\ 0 & \hat{\varepsilon}_{\mathbf{k}} - \mathrm{i}\frac{\lambda}{2}\hat{\varepsilon}^z & 0 & -\mathrm{i}\frac{\lambda'}{2}\hat{\varepsilon}^z \\ \hline \mathrm{i}\frac{\lambda'}{2}\hat{\varepsilon}^z & 0 & \hat{\varepsilon}_{\mathbf{k}+\mathbf{Q}_F} + \mathrm{i}\frac{\lambda}{2}\hat{\varepsilon}^z & 0 \\ 0 & -\mathrm{i}\frac{\lambda'}{2}\hat{\varepsilon}^z & 0 & \hat{\varepsilon}_{\mathbf{k}+\mathbf{Q}_F} - \mathrm{i}\frac{\lambda}{2}\hat{\varepsilon}^z \end{array}\right). \tag{18}$$

4. Results of the band structure and Fermi surface calculations

For $\lambda = 0$, the band structure and the Fermi surface are shown in Fig. 1. It is essentially the same as in Ref. [9] but within the folded BZ.

First, we switch on only the intercell SO interaction by setting $\lambda = 0$ and $\lambda' = 100$ meV. Corresponding band structure and the Fermi surface are shown in Fig. 2. There is a pronounced splitting between the previously degenerate electron M-pockets along the $X-M$ direction. Now, the band structure can not be unfolded. Also, there is a splitting between bands at M point and along the $M-\Gamma$ direction around -1 eV.

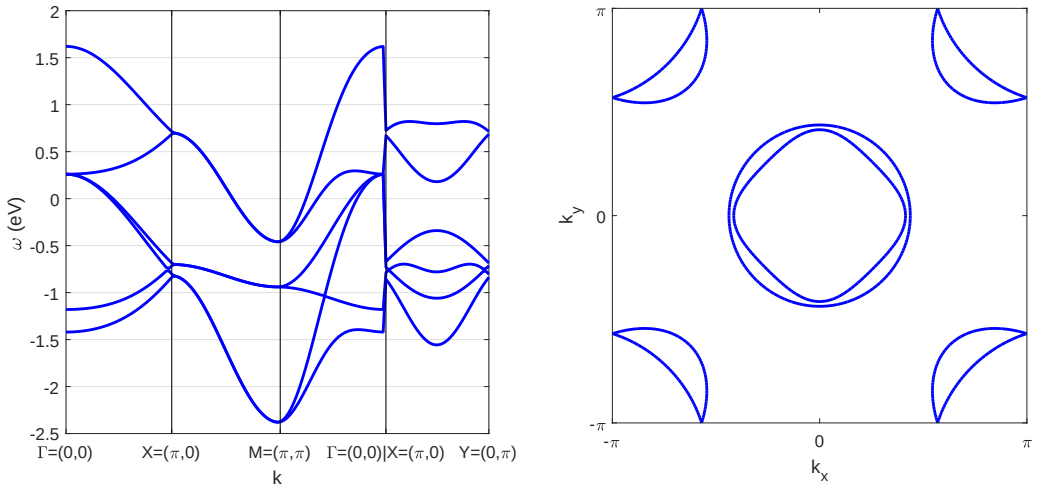

Fig. 1. Band structure and the Fermi surface in the three-orbital model without the SO coupling ($\lambda = \lambda' = 0$) in the 2-Fe BZ

Now we also switch on the intracell SO interaction by setting $\lambda = \lambda' = 100$ meV. The result is shown in Fig. 3. Apparently, the intracell SO coupling provides shift of the bands around Γ point. Apart from that, there is no pronounced difference between Fig. 2 and Fig. 3.

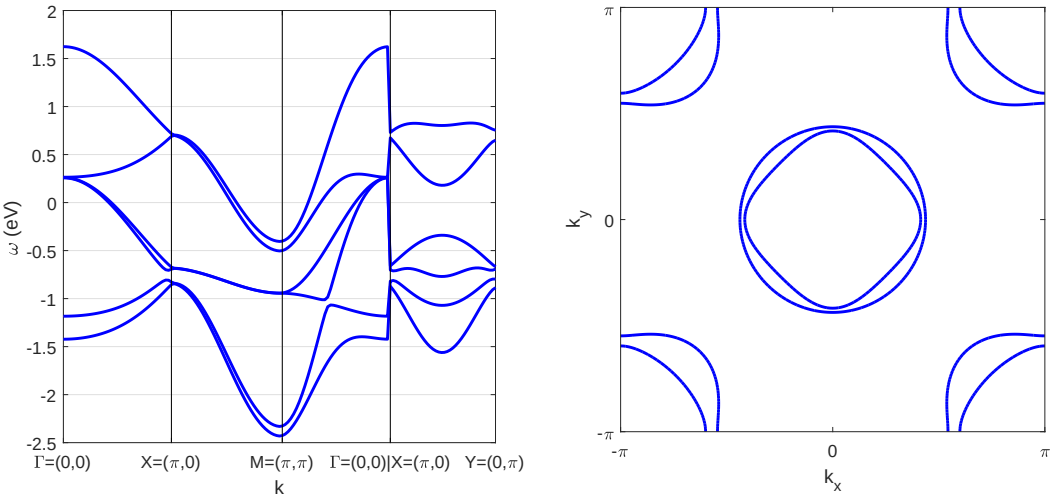

Fig. 2. The same as in Fig. 1 but for the finite intercell SO coupling $\lambda' = 100$ meV and the vanishing intracell SO coupling $\lambda = 0$

Conclusions

If working in the 2-Fe BZ, the SO coupling can be divided into the intra- and intercell parts, though both being local. We conclude that intercell coupling produces the reconstruction of the Fermi surface around the M point. The new band structure can not be unfolded anymore. Intracell SO coupling removes degeneracy of the bands around Γ point. There is also a splitting between bands at M point and along the $M-\Gamma$ direction around -1 eV. However, these energies are far below the chemical potential and should not affect the low-energy physics.

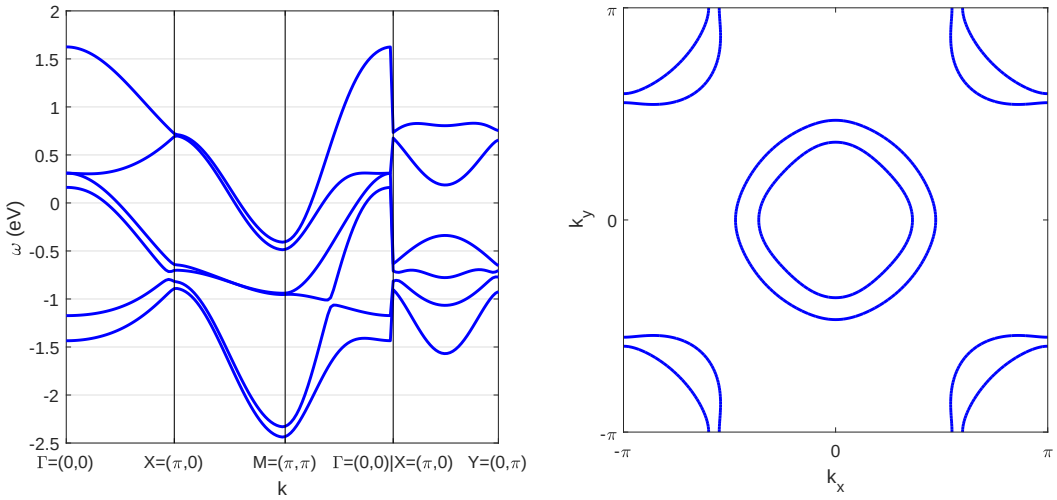

Fig. 3. The same as in Fig. 1 but for the finite intra- and intercell SO coupling, $\lambda = \lambda' = 100$ meV

This work was supported in part by the Russian Foundation for Basic Research (grant 16-02-00098) and BASIS Foundation for Development of Theoretical Physics and Mathematics.

References

[1] P.J.Hirschfeld, M.M.Korshunov, I.I.Mazin, Gap symmetry and structure of Fe-based superconductors, *Rep. Prog. Phys.*, **74**(2011), 124508.

[2] M.M.Korshunov, I.Eremin, Doping evolution of itinerant magnetic fluctuations in Fe-based pnictides, *Europhys. Lett.*, **83**(2008), 67003.

[3] I.I.Mazin, D.J.Singh, M.D.Johannes, M.-H.Du, Unconventional Superconductivity with a Sign Reversal in the Order Parameter of $LaFeAsO_{1-x}F_x$, *Phys. Rev. Lett.*, **101**(2008), 057003.

[4] S.Graser, T.A.Maier, P.J.Hirschfeld, D.J.Scalapino, Near-degeneracy of several pairing channels in multiorbital models for the Fe pnictides, *New. J. Phys.*, **11**(2009), 025016.

[5] K.Kuroki, S.Onari, R.Arita, H.Usui, Y.Tanaka, H.Kontani, H.Aoki, Unconventional Pairing Originating from the Disconnected Fermi Surfaces of Superconducting $LaFeAsO_{1-x}F_x$, *Phys. Rev. Lett.*, **101**(2008), 087004.

[6] S.Maiti, M.M.Korshunov, T.A.Maier, P.J.Hirschfeld, A.V.Chubukov, Evolution of the Superconducting State of Fe-Based Compounds with Doping, *Phys. Rev. Lett.*, **107**(2011), 147002.

[7] M.M.Korshunov, Superconducting state in iron-based materials and spin-fluctuation pairing theory, *Physics-Uspekhi*, **57**(2014), 813.

[8] S.Raghu, X.-L.Qi, C.-X.Liu, D.J.Scalapino, S.-C.Zhang, Minimal two-band model of the superconducting iron oxypnictides, *Phys. Rev. B*, **77**(2008), 220503.

[9] M.M.Korshunov, Y.N.Togushova, I.Eremin, Three-orbital model for Fe-pnictides, *J. Supercond. Nov. Magn.*, **26**(2013), 2665.

[10] O.J.Lipscombe, L.W.Harriger, P.G.Freeman, M.Enderle, C.Zhang, M.Wang, T.Egami, J.Hu, T.Xiang, M.R.Norman, P.Dai, Anisotropic neutron spin resonance in superconducting $BaFe_{1.9}Ni_{0.1}As_2$, *Phys. Rev. B*, **82**(2010), 064515.

[11] I.Eremin, D.Manske, K.H.Bennemann, Electronic theory for the normal-state spin dynamics in Sr_2RuO_4: Anisotropy due to spin-orbit coupling, *Phys. Rev. B*, **65**(2002), 220502(R).

[12] M.M.Korshunov, Y.N.Togushova, I.Eremin, P.J. Hirschfeld, Spin-orbit coupling in Fe-based superconductors, *J. Supercond. Nov. Magn.*, **26**(2013), 2873.

[13] K.K.Ng, M.Sigrist, *Europhys. Lett.*, **49**(2000), 473.

[14] L.H.Ryder, Quantum Field Theory, *Cambridge University Press*, 2nd edition, 1996.

Изменение зонной структуры из-за спин-орбитального взаимодействия в трехорбитальной модели пниктидов железа

Максим М. Коршунов
Сибирский федеральный университет
Свободный, 79, Красноярск, 660041
Институт физики им. Л. В. Киренского ФИЦ КНЦ СО РАН
Академгородок, 50/38, Красноярск, 660036
Россия

Юлия Н. Тогушова
Сибирский федеральный университет
Свободный, 79, Красноярск, 660041
Россия

Исследовано влияние спин-орбитального взаимодействия на зонную сруктуру и поверхность Ферми трехорбитальной модели в зоне Бриллюэна двух атомов железа на ячейку. Из-за присутствия двух атомов железа в кристаллографической элементарной ячейке спин-орбитальное взаимодействие можно разделить на внутри- и межъячеечную части по отношению к элементарной ячейке решетки железа. Показано, что межъячеечная часть приводит к реконструкции поверхности Ферми в виде выраженного расщепления между ранее вырожденными электронными карманами в точке (π, π) *вдоль направления* $(0, \pi) - (\pi, \pi)$*. Внутриячеечная часть приводит к сдвигу зон вблизи точки* $(0, 0)$ *и снимает там вырождение. Также имеют место другие сдвиги зон, но они не должны влиять на низкоэнергетическую физику, поскольку возникают на энергиях порядка 1 eV ниже уровня Ферми.*

Ключевые слова: сверхпроводники на основе железа, спин-орбитальное взаимодействие, зонная структура, поверхность Ферми.